

Solar Source Regions of Space Weather Events

Bhuwan Joshi

Udaipur Solar Observatory

Physical Research Laboratory, India



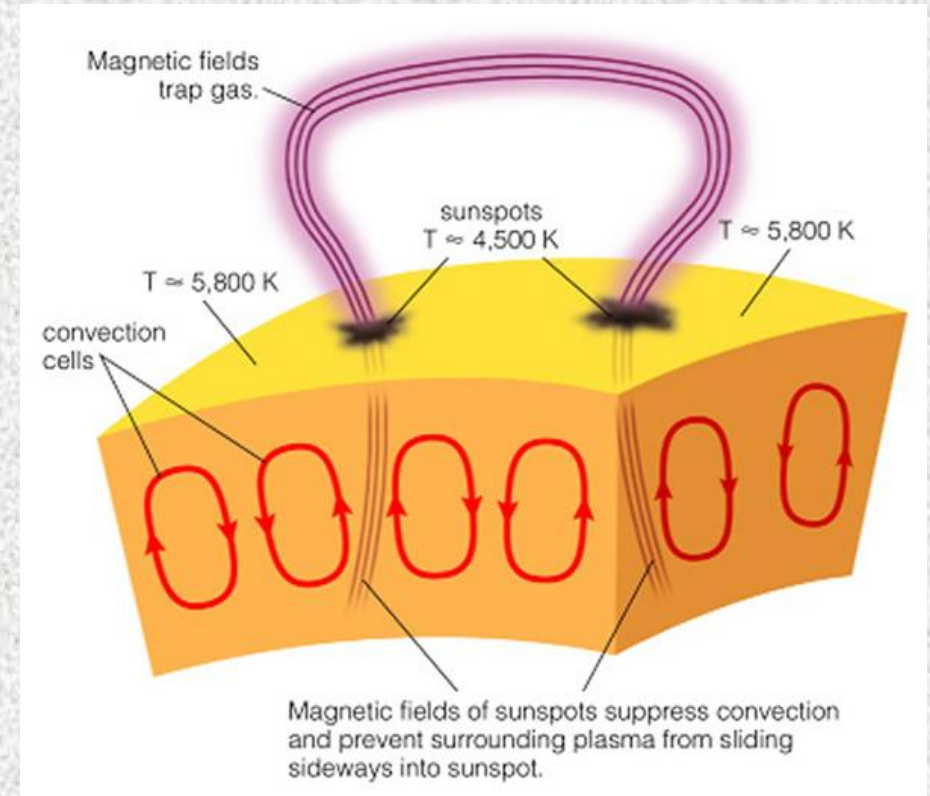
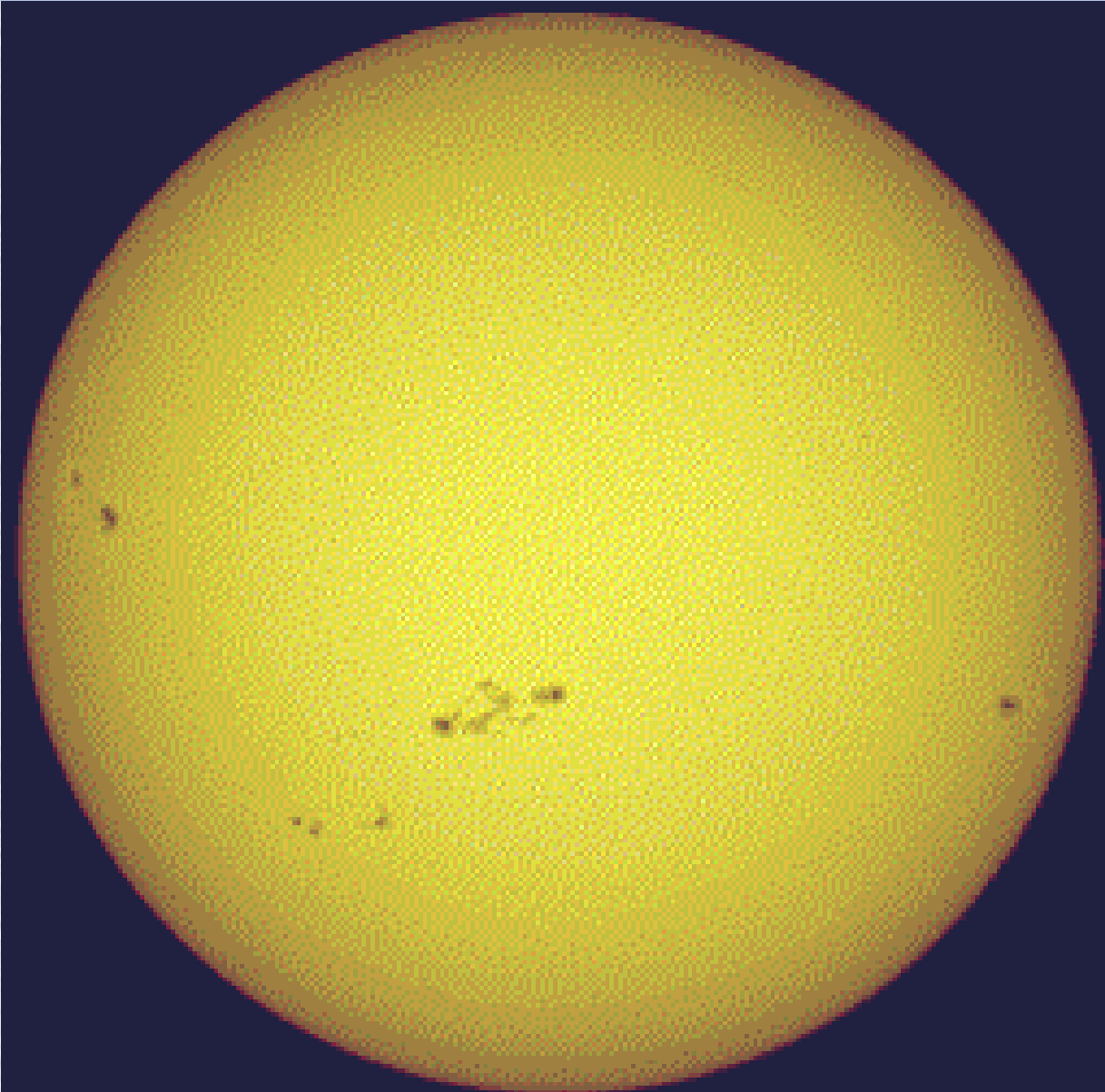
The International Space Weather Initiative Workshop on Space Weather

3/11/2021

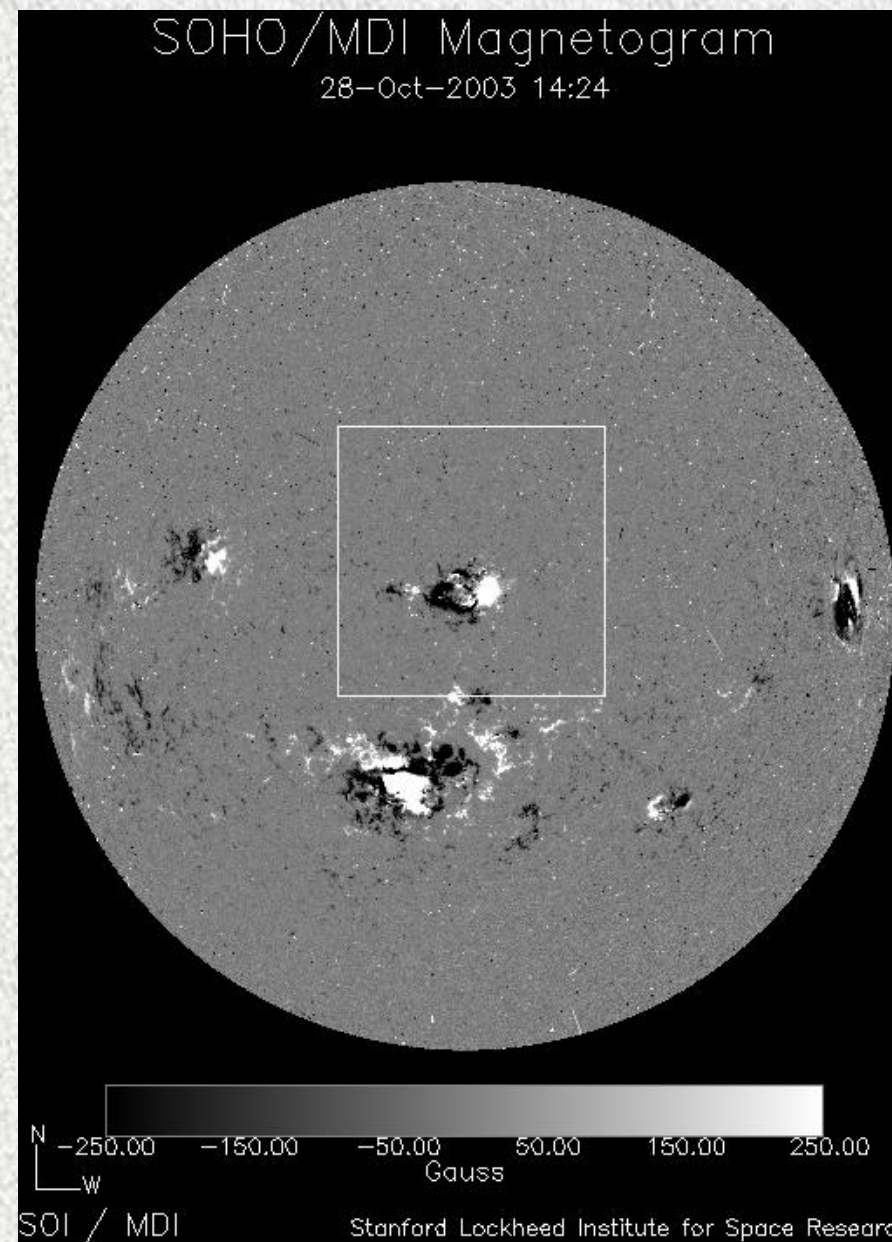
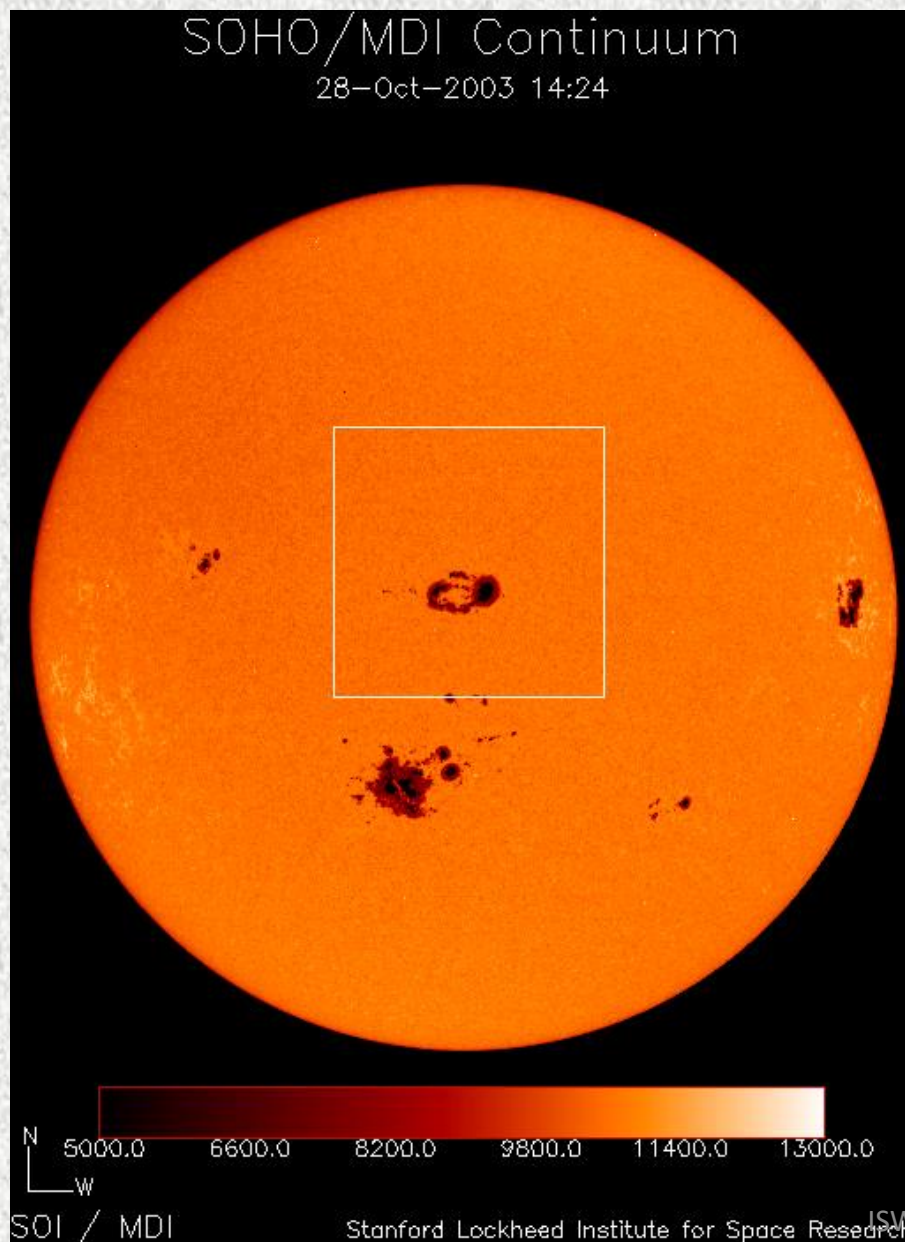
Science and Applications

Solar active regions

Source regions of coronal transients



Solar Active Regions: *While light and magnetogram images*

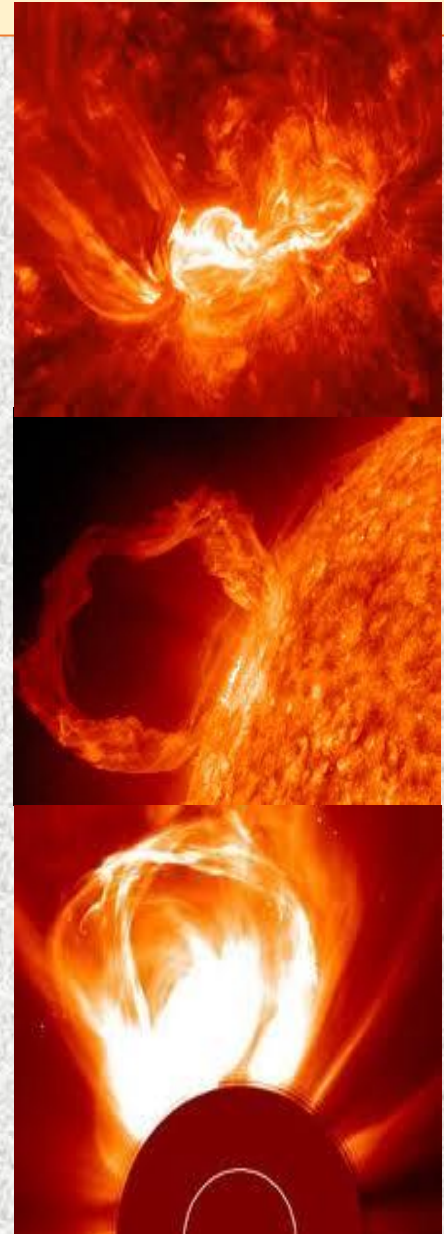


Coronal Transients: Source of Solar Storms

Solar Eruptive Phenomena correspond to the various kinds of *transient magnetic activities* occurring in the solar atmosphere in the form of

- ❖ **Solar Flares**
- ❖ **Prominence/filament eruptions**
- ❖ **Coronal Mass Ejections (CMEs)**

The above phenomena are strongly coupled to each other



Solar Flares

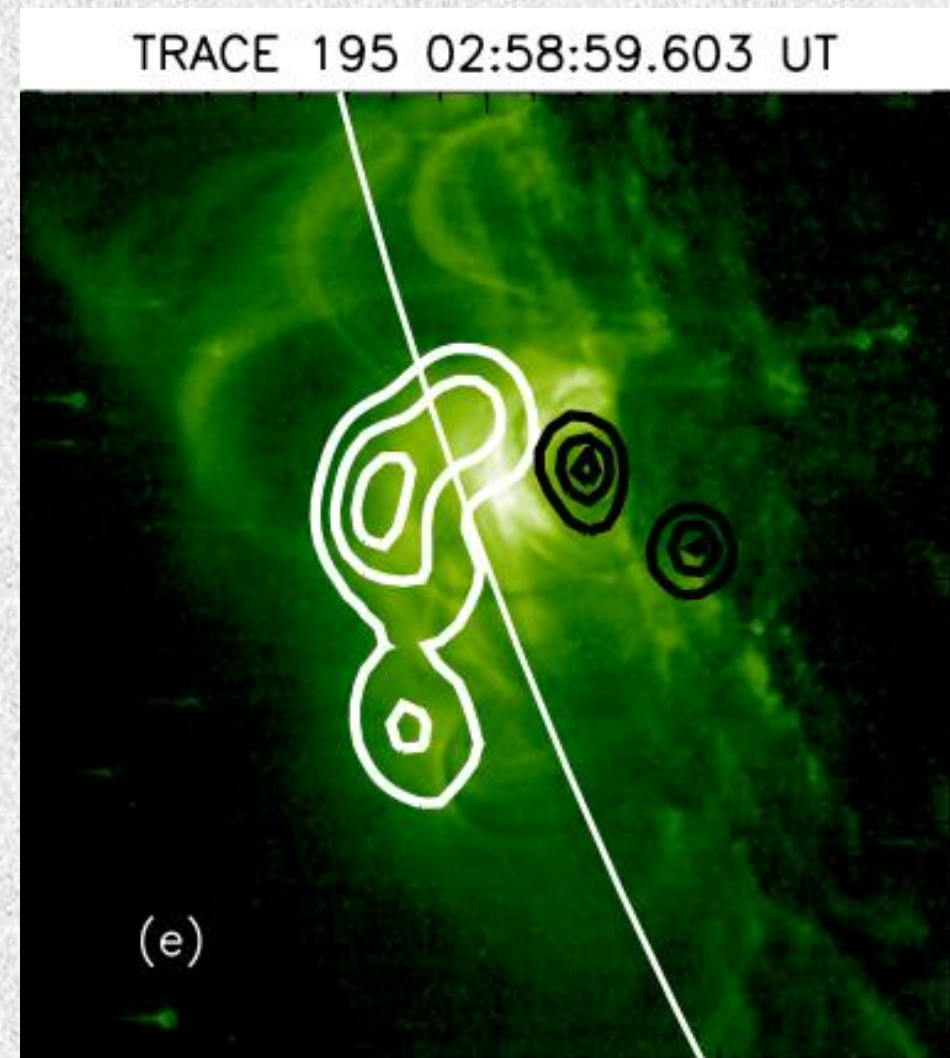
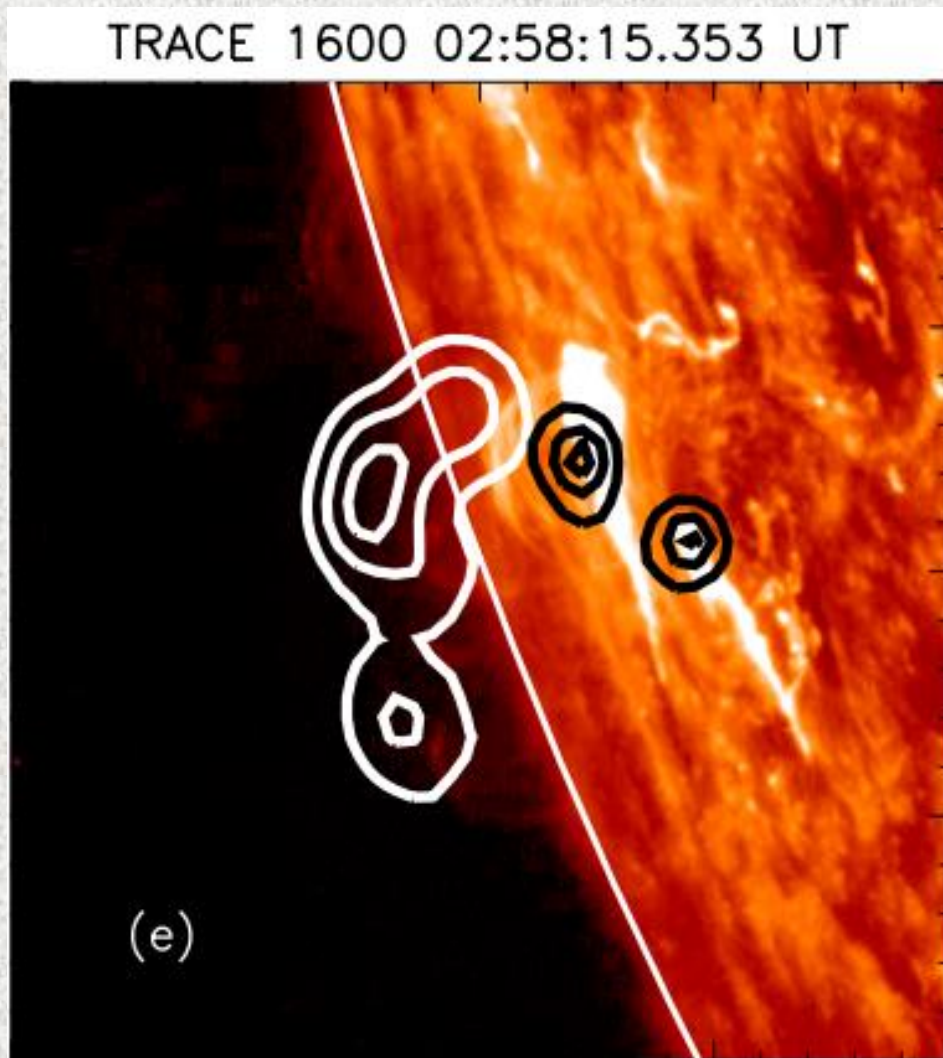
- ❑ Transient, explosive perturbations in the solar atmosphere (in excess of 10^{32} erg)
- *Millions of 100-megaton hydrogen bombs exploding at the same time! (The energy released in the explosion of one megaton of TNT is equal to 4.2×10^{22} ergs.)*
- *Ten million times greater than the energy released from a volcanic explosion.*

❑ **Confined & Eruptive**

❑ **Magnetic reconnection**

Scenario of "standard flare"

(Joshi et al. 2009, ApJ)

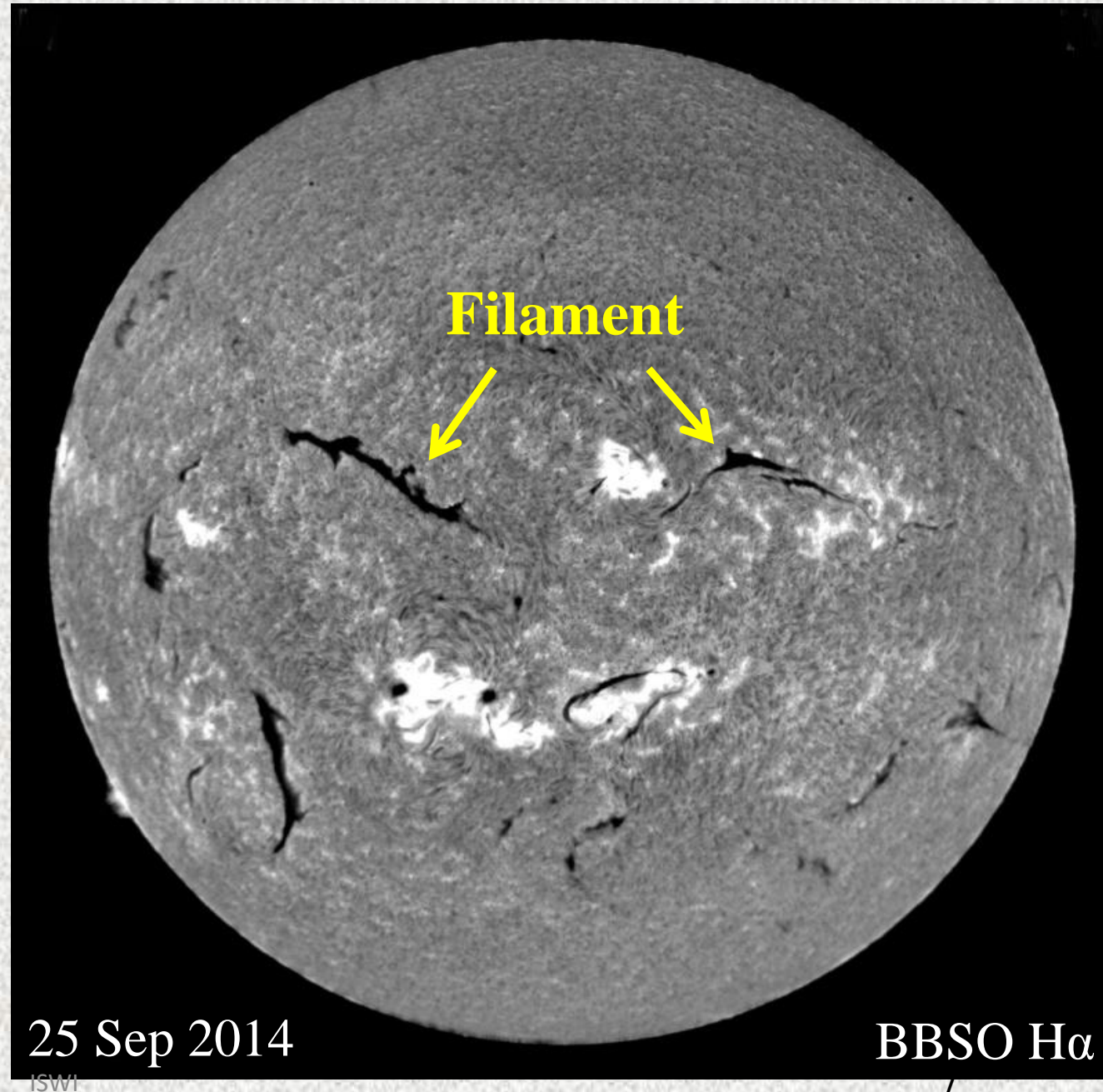


Foot-point and loop-top sources

Solar filaments

- Solar filaments are large magnetic structures confining a cool and dense plasma in the solar corona
 - $T \sim 10^4$ K; $n_e \sim 10^{17} m^{-3}$
- Coronal values
($n_e \sim 10^{15} m^{-3}$; $T \sim 10^6$ K)
- Termed as 'Prominences' when observed above the solar limb, appear as bright features.

Credit: <https://www.swpc.noaa.gov>
3/11/2021

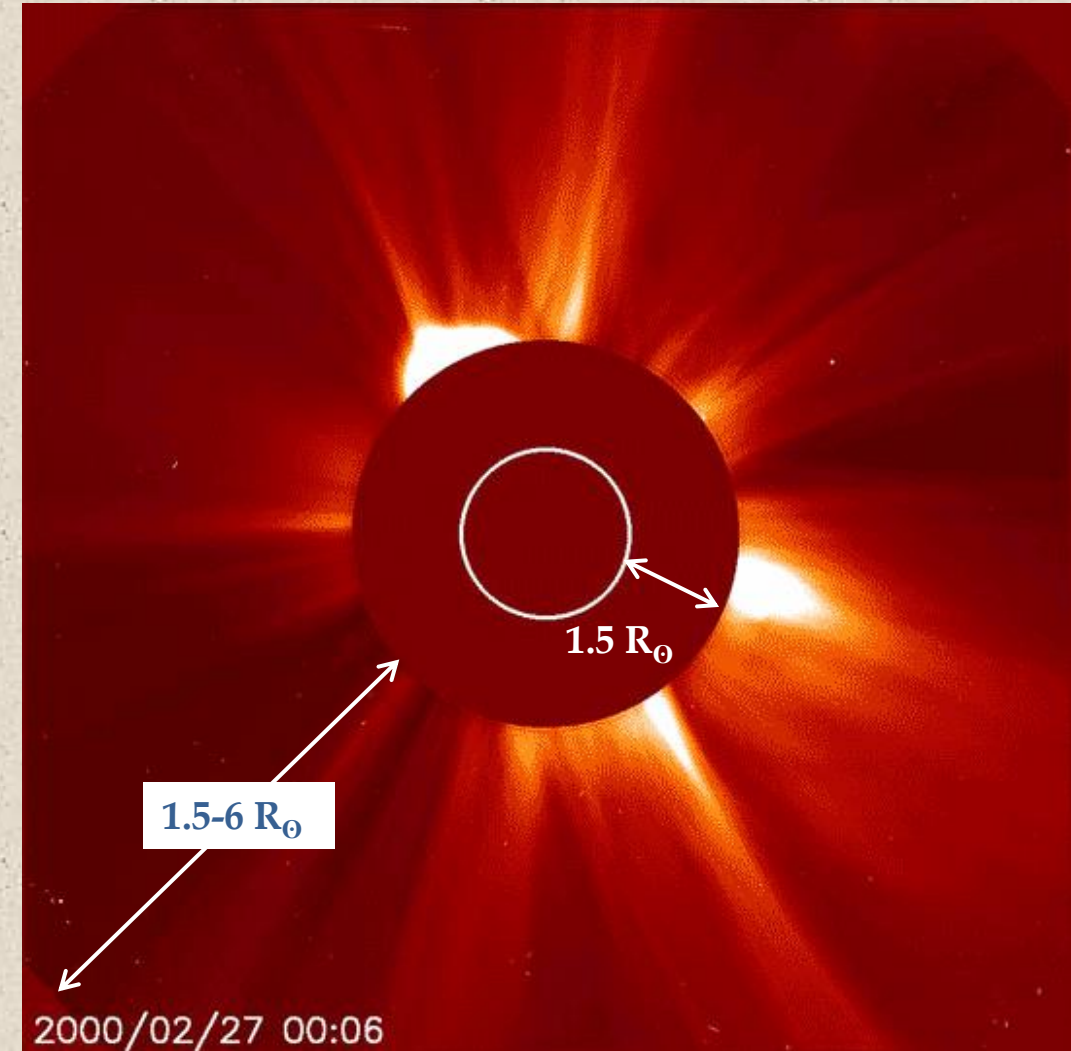


Coronal Mass Ejections

- CMEs consist of large structures containing plasma and magnetic fields that are expelled from the Sun into the heliosphere.

| Parameters | Value |
|----------------|---|
| Speed | Few km s^{-1} to $> 3000 \text{ km s}^{-1}$ |
| Mass | 10^{12} to 10^{13} kg |
| Kinetic energy | 10^{23} to 10^{24} J |
| Angular width | 2° to 360° ; Average $\approx 47^\circ$ 360° : Halo CME |

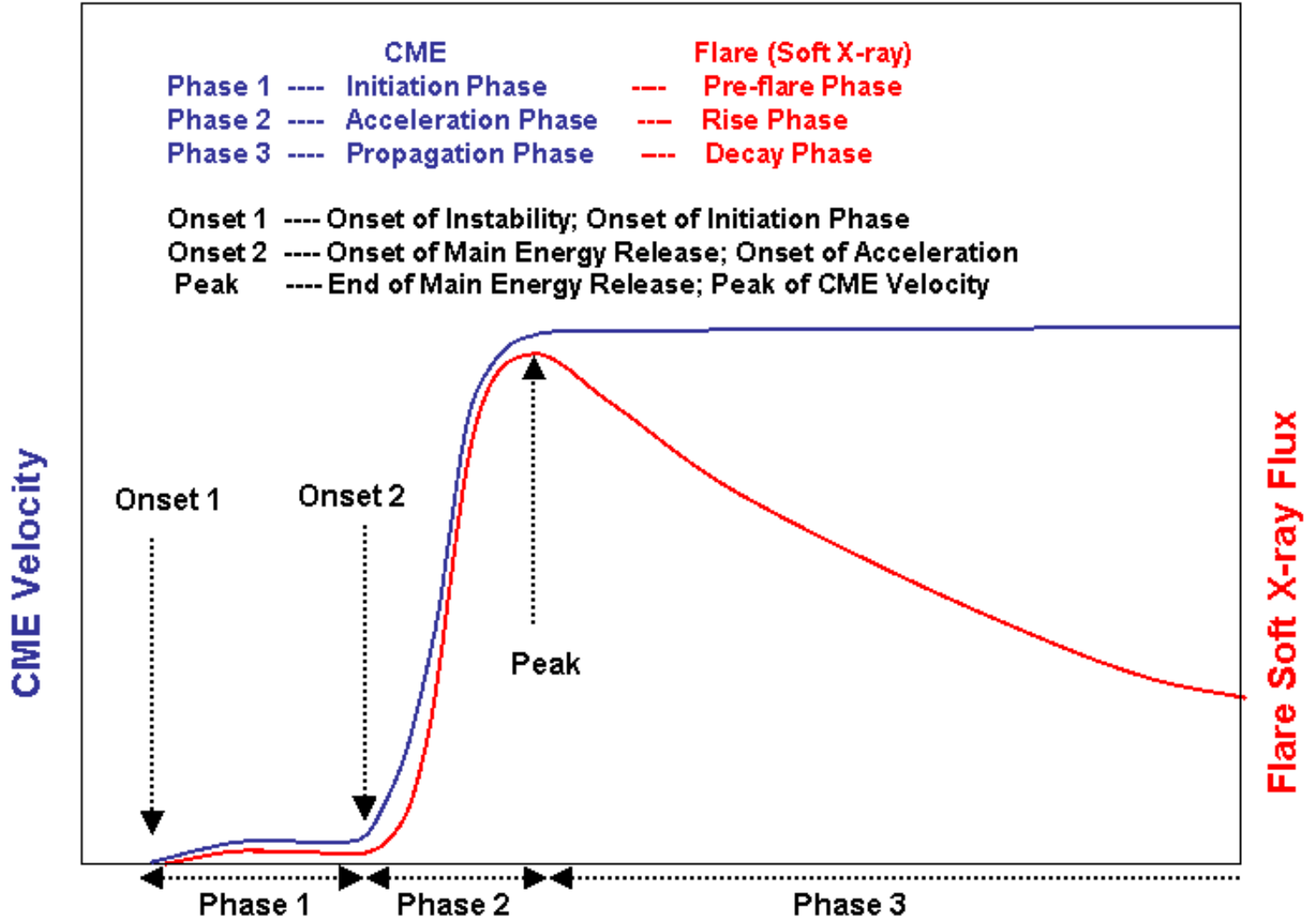
Webb & Howard, 2012



From SOHO/LASCO archive

Onset of CME and flare-CME association

CME Kinematic Evolution and Timing with Associated Flare

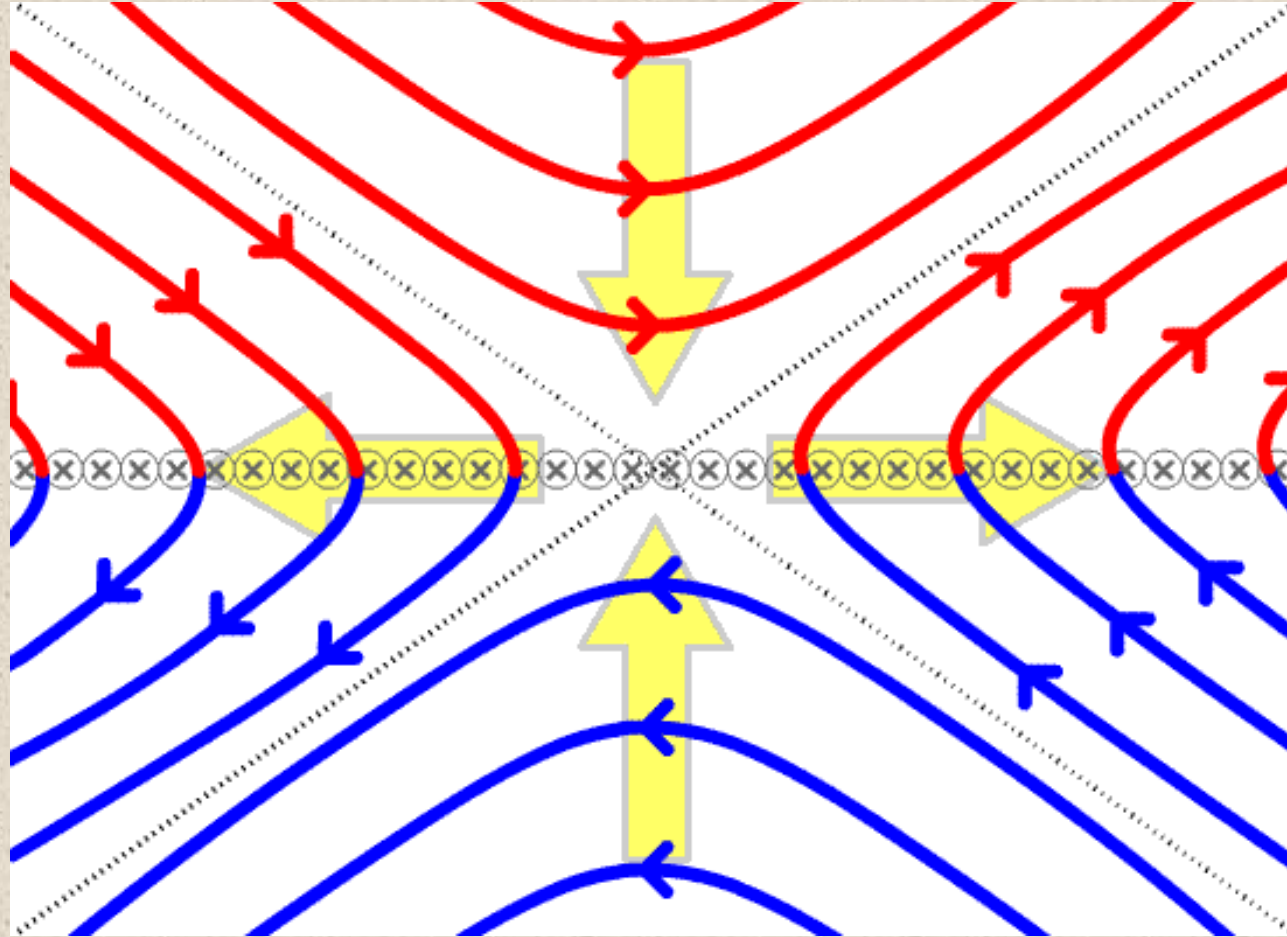


Temporal coincidence between CME acceleration and flare flux



CME eruption is strongly coupled with the magnetic reconnection process that causes the flare

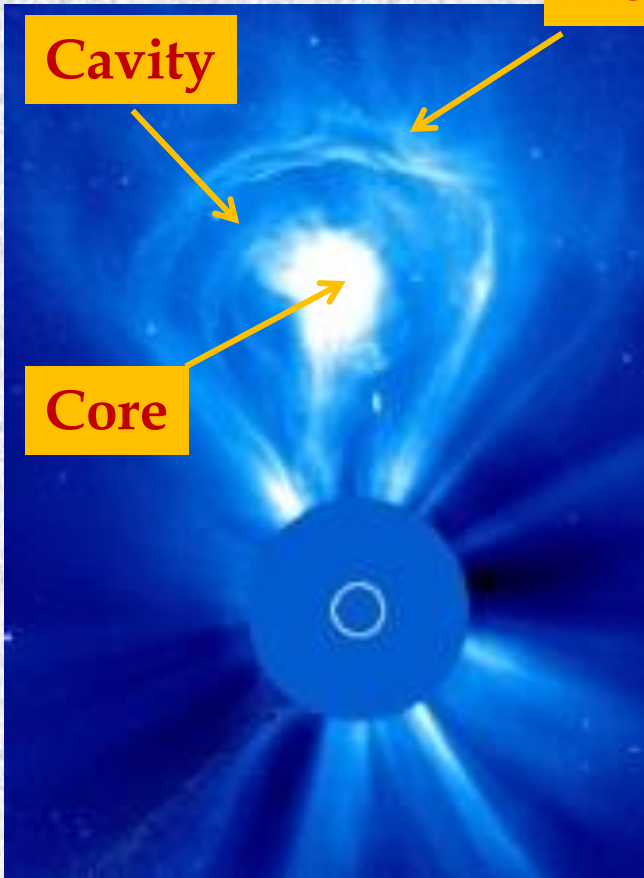
How does impulsive energy release take place?



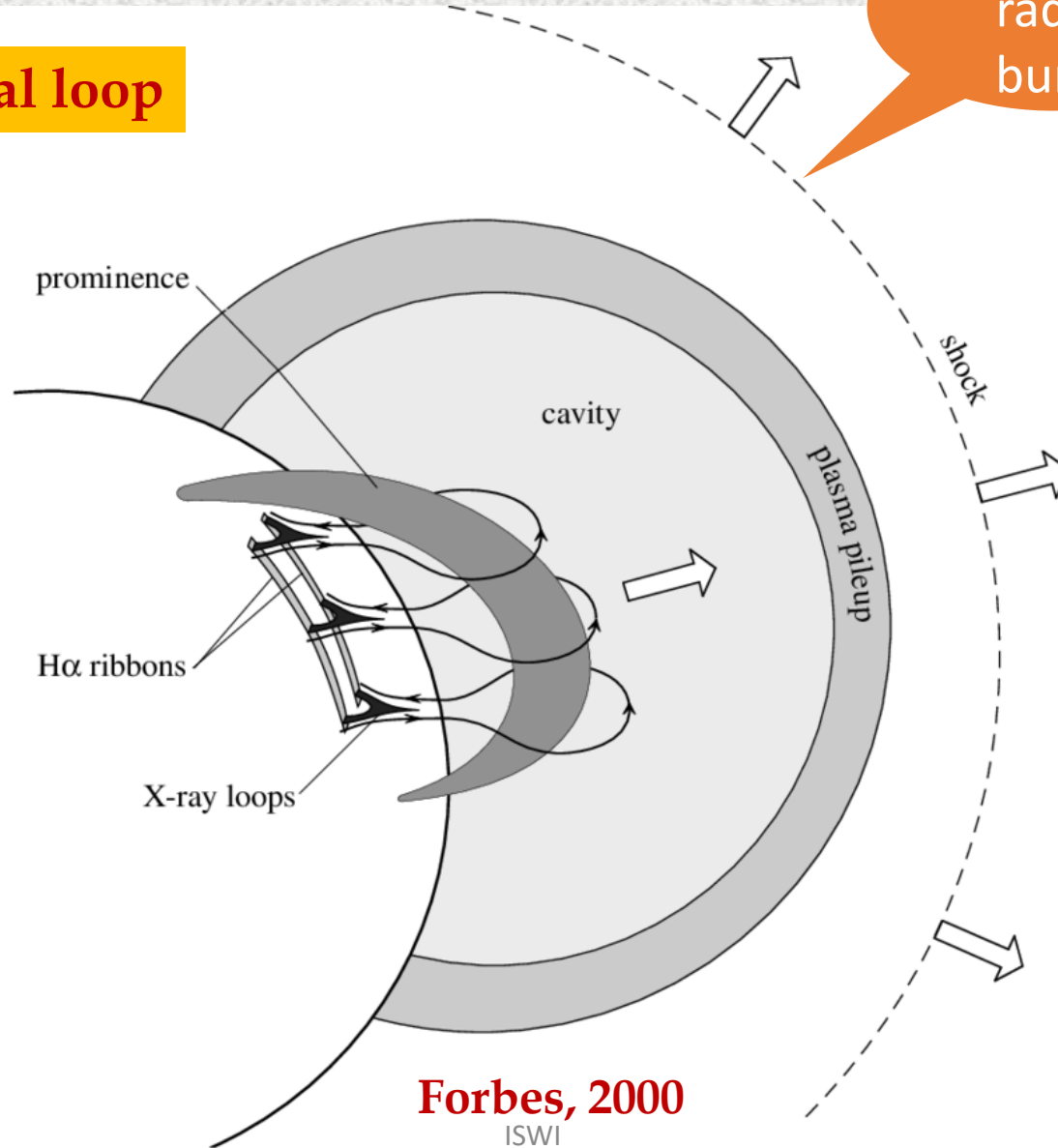
Animation courtesy
en.wikipedia.org

Magnetic reconnection: Breaking and topological rearrangement of oppositely directed magnetic field lines in a plasma; magnetic field energy is converted to plasma kinetic and thermal energy.

Classical 3-part CME structure



Frontal loop



Type II
radio
burst

Bright frontal loop

Plasma pile-up

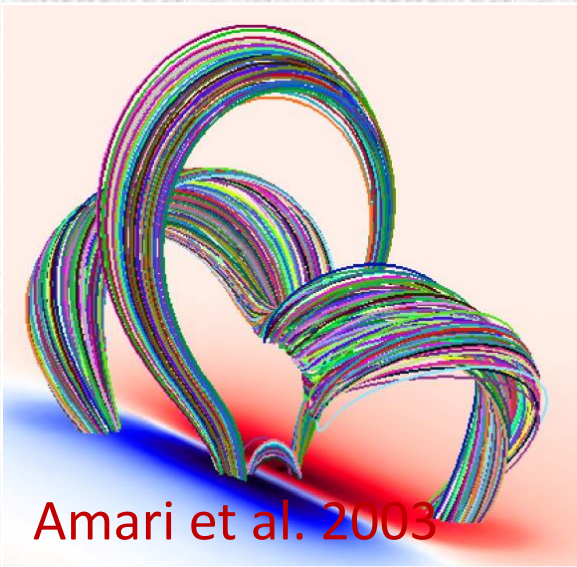
Cavity

Reduced density
(fluxrope)

Core

Prominence

Magnetic Flux Rope



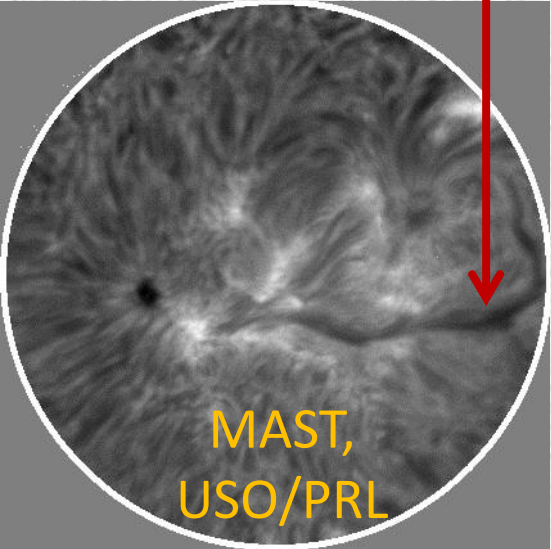
❖ A set of twisted magnetic field lines wrapped around its central axis.
(Gibson & Fan 2006)

Observational counterparts

Active region filaments

Coronal cavities

Coronal hot channels



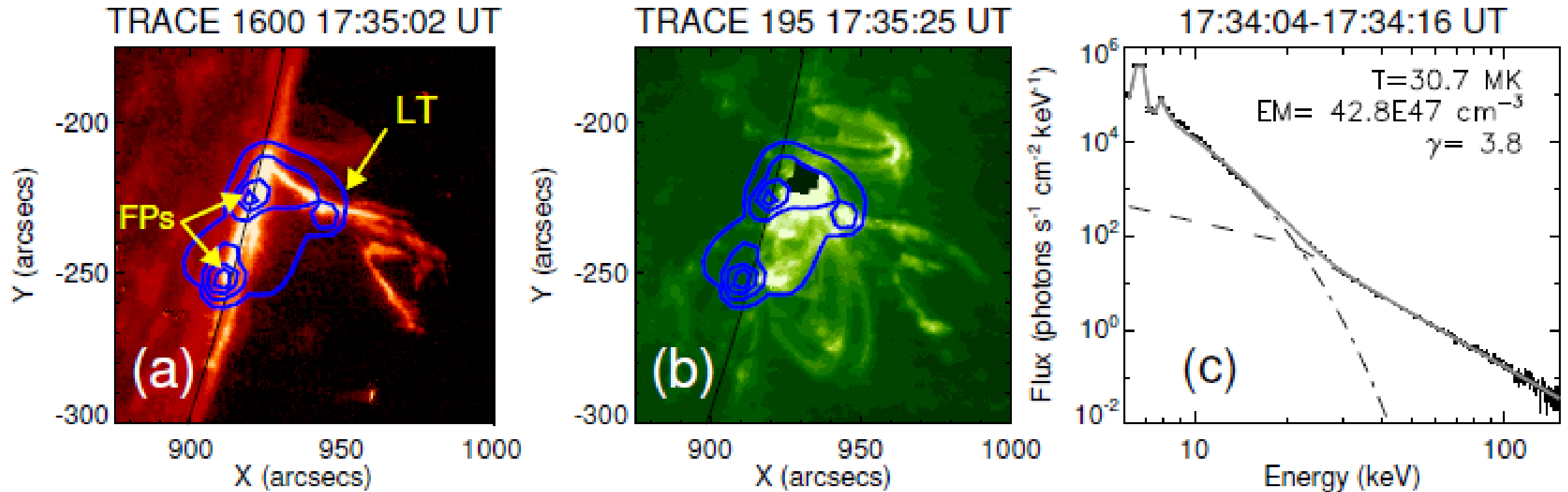
Flares and CMEs: Open questions

- ❖ **What is the most likely magnetic configuration in the pre-eruption phase (sigmoids, high magnetic helicity, newly emerging flux)?**
- ❖ **What fraction of the energy released in flares goes into accelerating electrons and what fraction goes directly into heating electrons?**
- ❖ **Where does this heating and acceleration occur?**
- ❖ **How are electrons accelerated to high energies and heated to high temperatures?**
- ❖ **How do CME initiate and evolve?**

Non-thermal emission from coronal sources

(Joshi et al. 2013, ApJ)

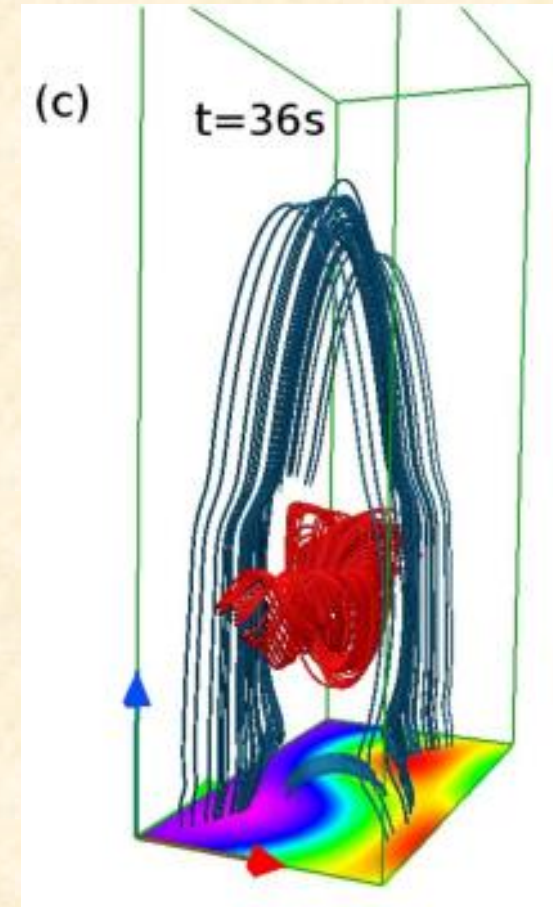
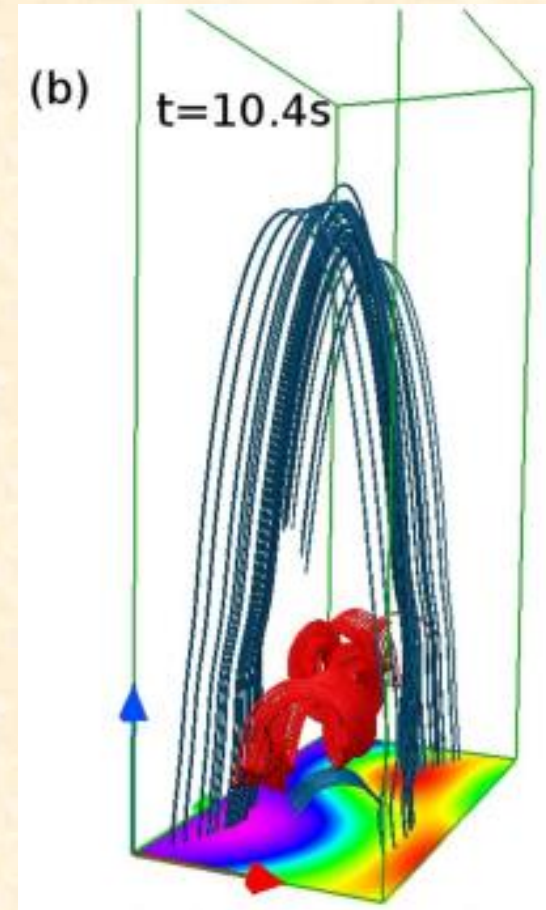
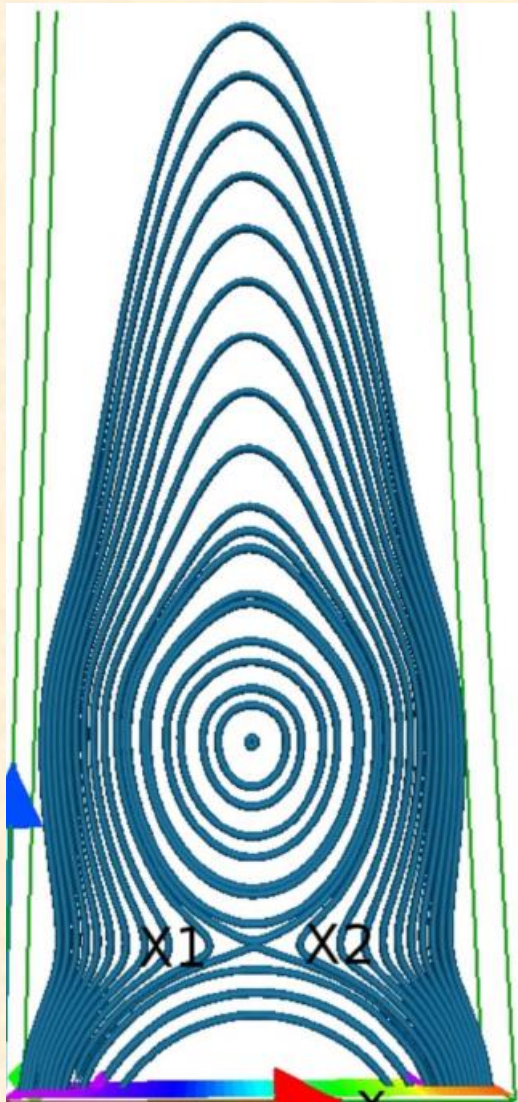
Blue contours: 50-100 keV HXR source



□ Unambiguous detection of high energy coronal HXR source while the prominence gets detached during X1.8 flare on 18-August-2004

□ Location, timing, strength and spectrum of hard X-ray emission are indirect diagnostics of reconnection and particle acceleration.

Role of magnetic reconnection (Kumar S. et al. 2016, ApJ)



□ In-situ development of a Magnetic Flux Rope (MFR)

3/11/2021

ISWI

Energy budget

Thermal vs non-thermal energy

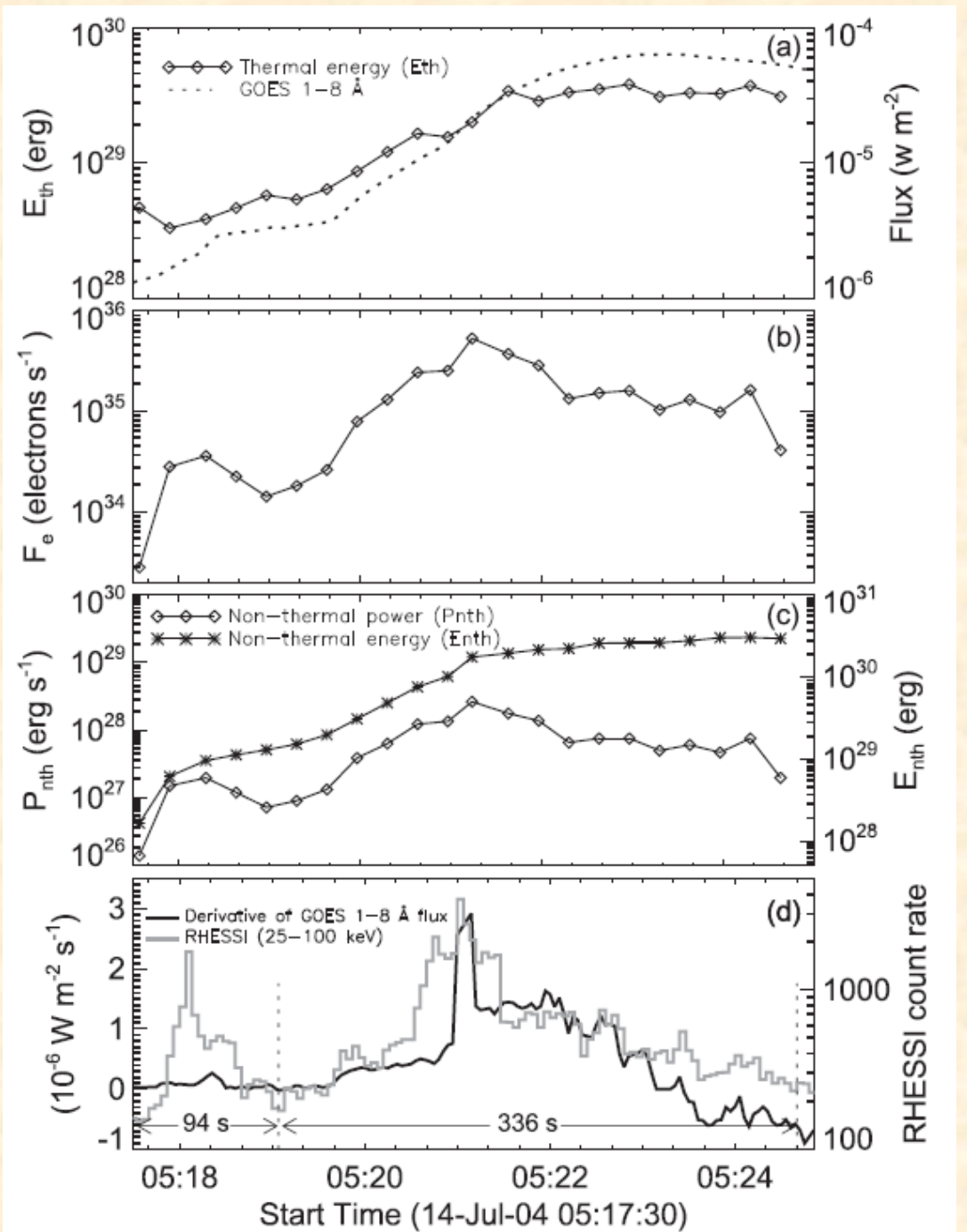
(Kushwaha et al. 2015, ApJ)

| Flare characteristics | Parameters |
|--|---------------------------|
| Duration of HXR impulsive phase | 430 s |
| No. of HXR peaks | 2 |
| | 94 s and 336 s |
| Total non-thermal energy $((E_{nth})_{tot})$ | 3.03×10^{30} erg |
| Thermal energy (E_{th}) | |
| -Thermal energy $(E_{th})_{max}$ | 3.89×10^{29} erg |
| -Thermal energy $(E_{th})_{min}$ | 0.33×10^{29} erg |
| $(E_{nth})_{tot}/(E_{th})_{max}$ | ~ 7.5 |

Nupert effect: Efficient conversion of non-thermal to thermal energy

$$E_{th} = 3k_B T n V = 3k_B T \sqrt{EM \cdot f \cdot V} \text{ [erg]}$$

$$P_{nth}(E > E_{LC}) = \frac{\delta - 1}{\delta - 2} F_e E_{LC} 10^{35} \text{ [erg s}^{-1}\text{]}$$



Solar Observing Facilities

Multi-Application Solar Telescope

Telescope & Observing floor

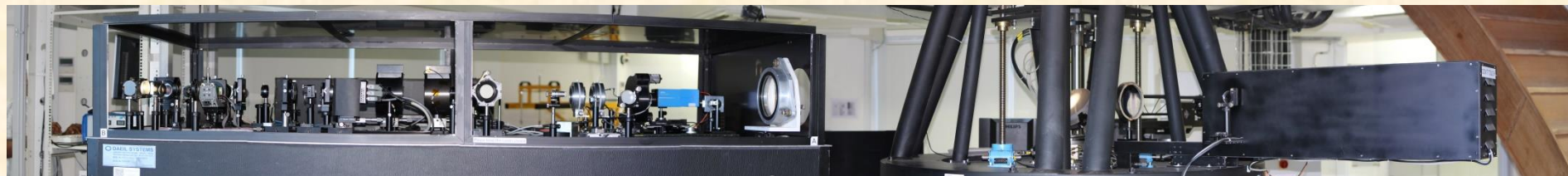
Telescope floor



Telescope enclosed with in the collapsible dome

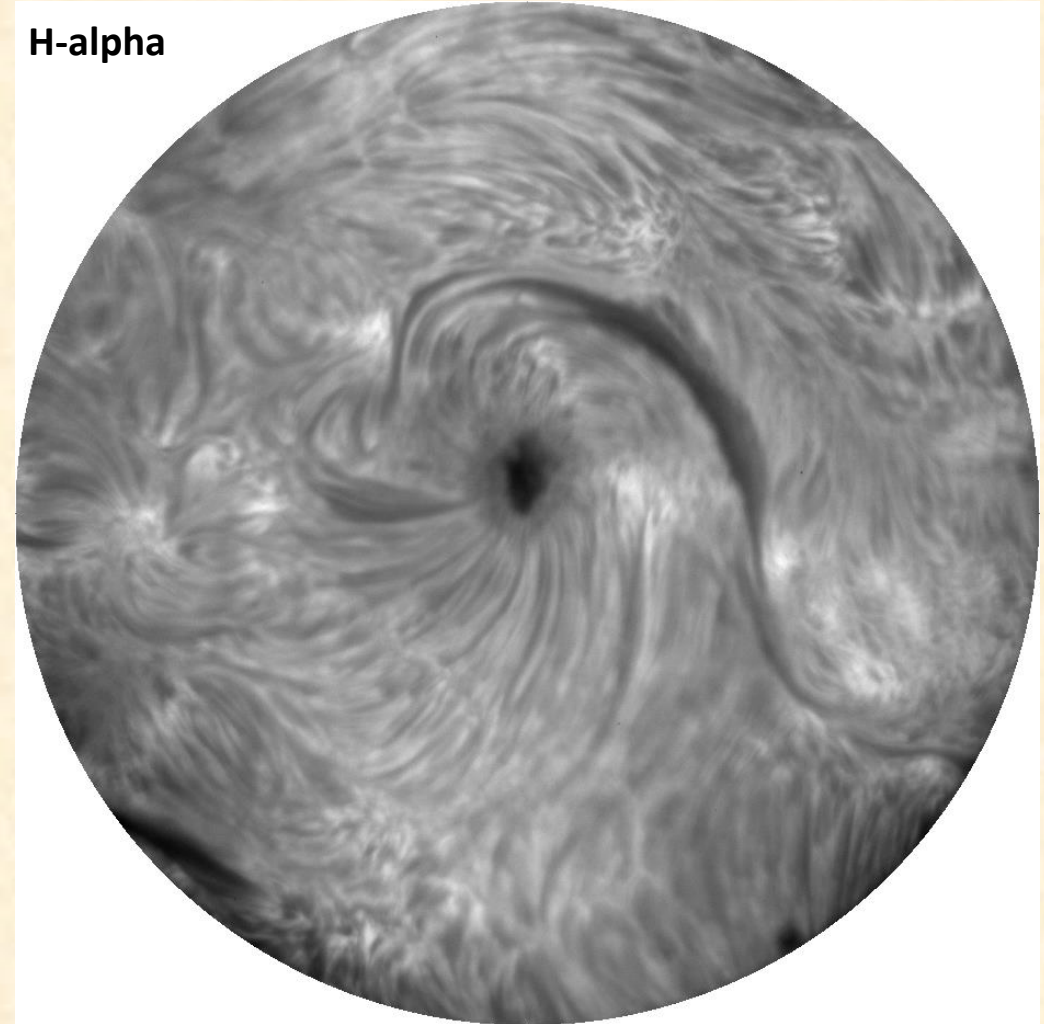
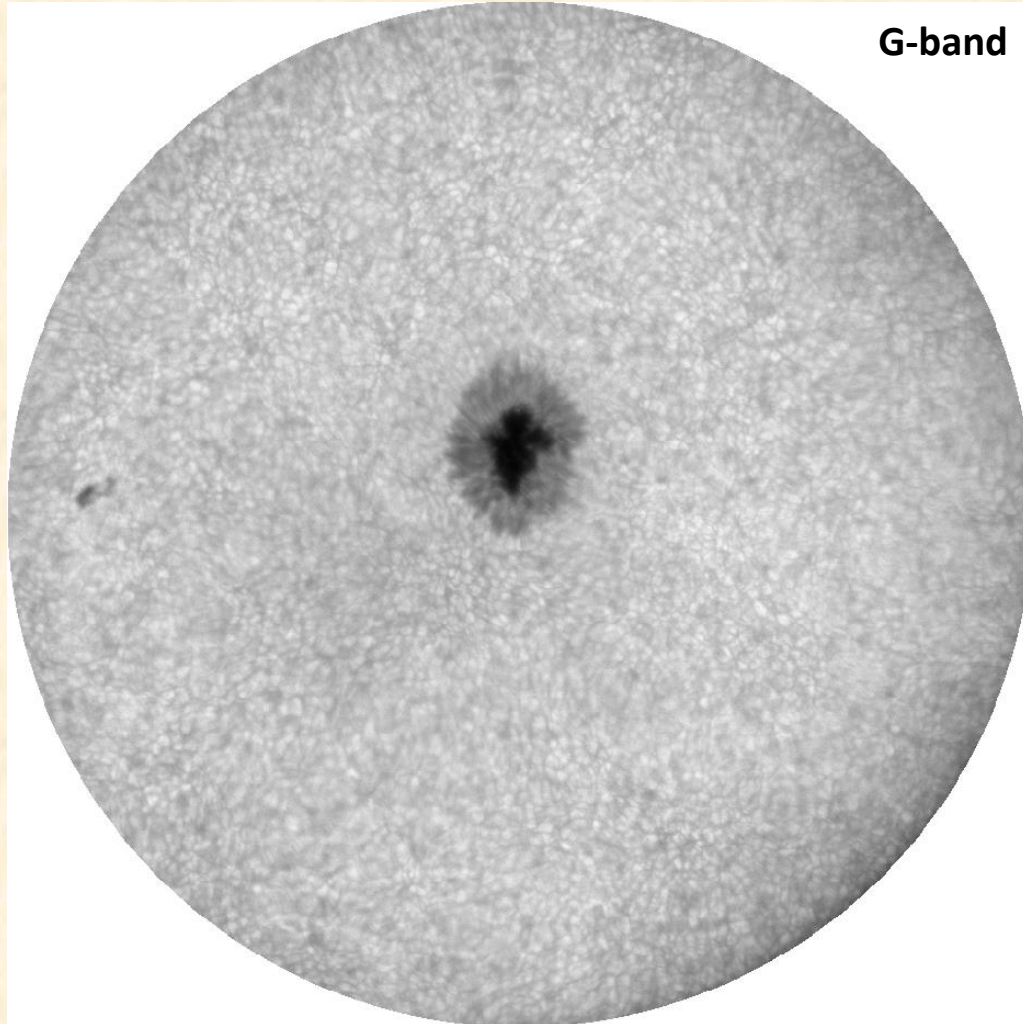


Back-end instruments on the observing floor



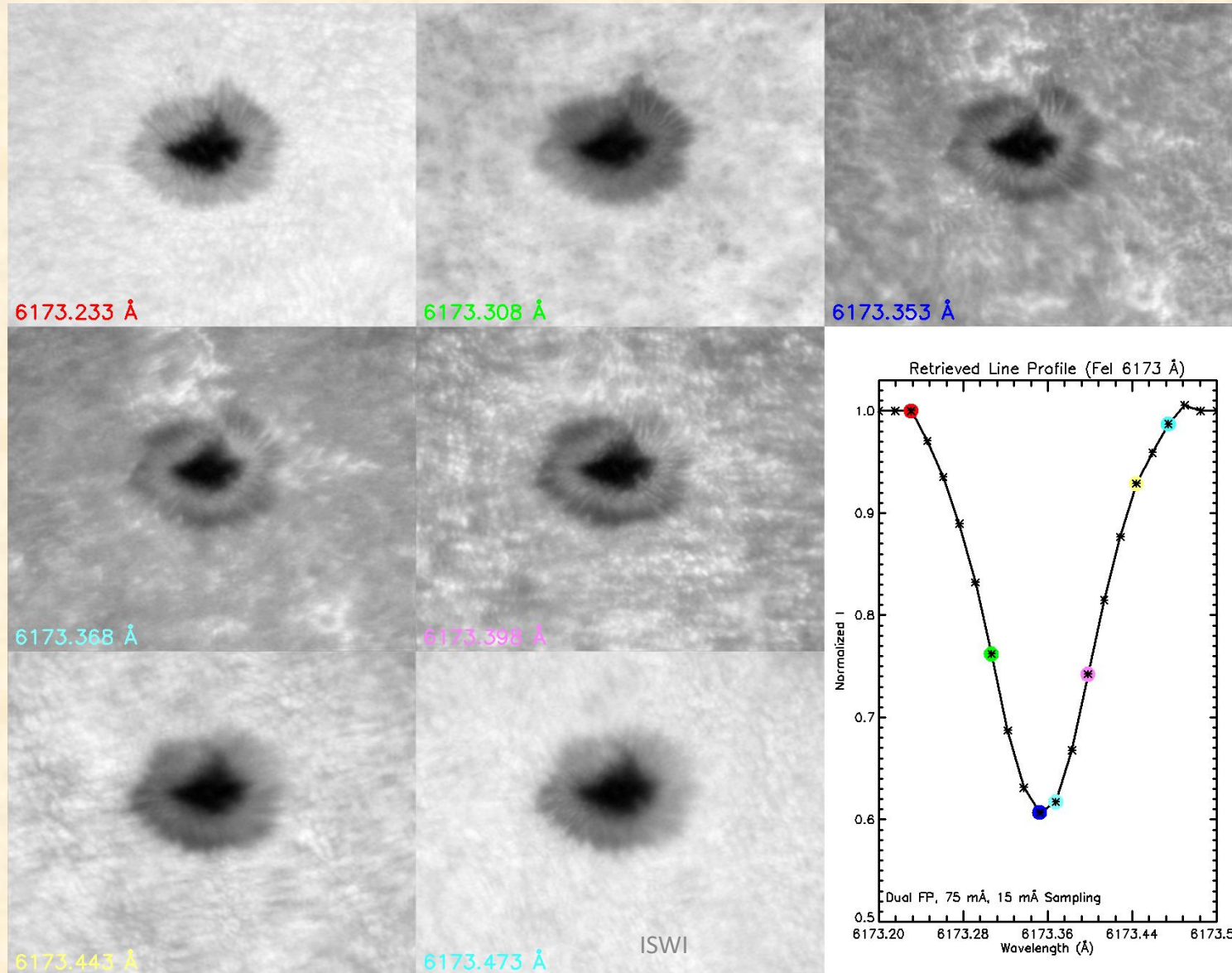
Multi-Application Solar Telescope

G-band and H-alpha sample images



Multi-Application Solar Telescope

Back-end instruments



Fabry-Perot Narrow band imager; typical tuning result: 22 Wavelength positions along the 617.3 nm line profile with 15 mÅ steps

CALLISTO solar radio spectrometer at USO-PRL, Udaipur

Commissioned in October 4, 2018

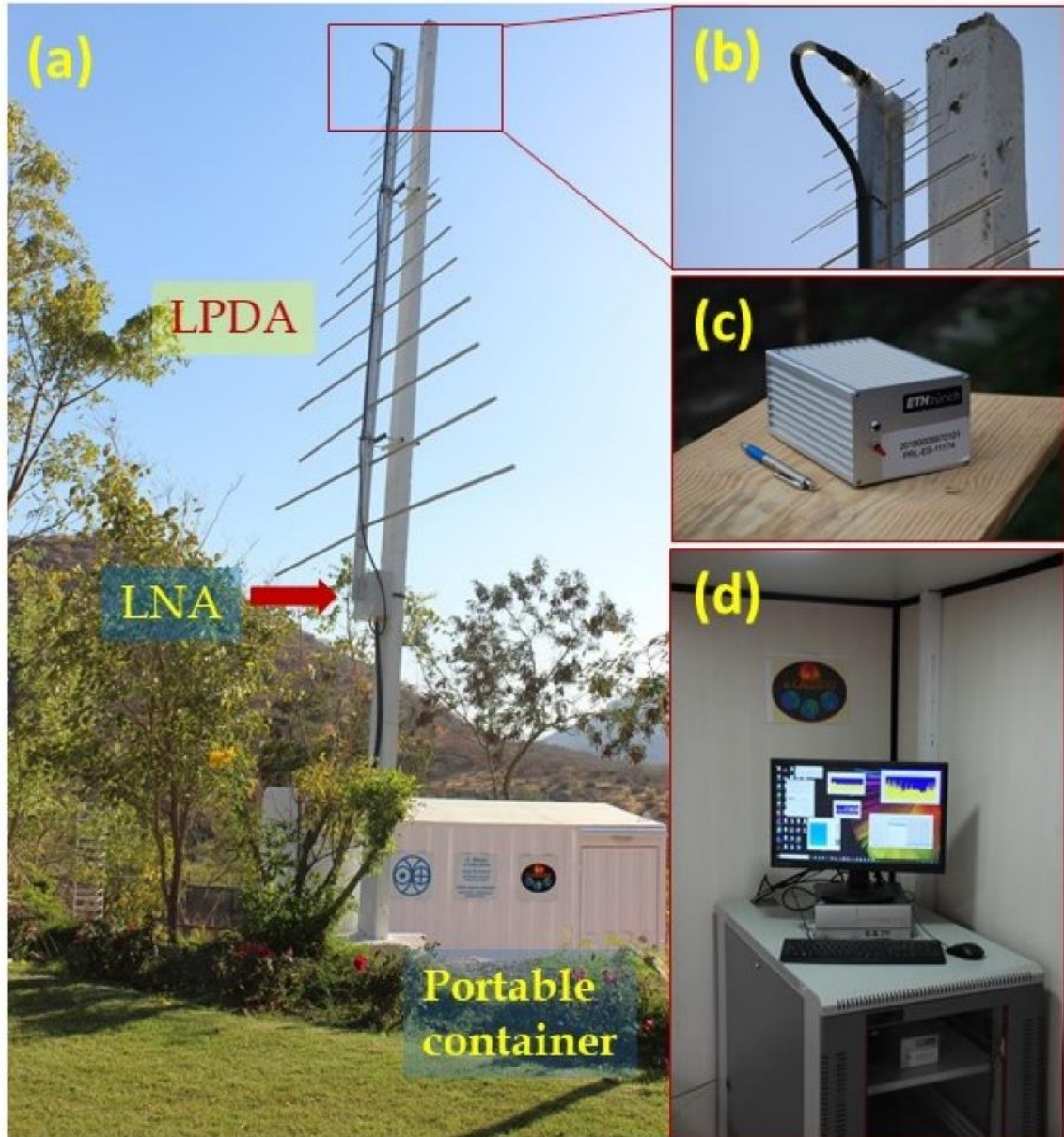


What is CALLISTO ?

| | |
|----------|-----------------|
| C | ompound |
| A | Stronomical |
| L | ow cost |
| L | ow frequency |
| I | nstrument for |
| S | pectroscopy and |
| T | ransportable |
| O | bservatory |

<http://www.e-callisto.org/>

Various subsystems of *Udaipur CALLISTO*



LPDA specifications

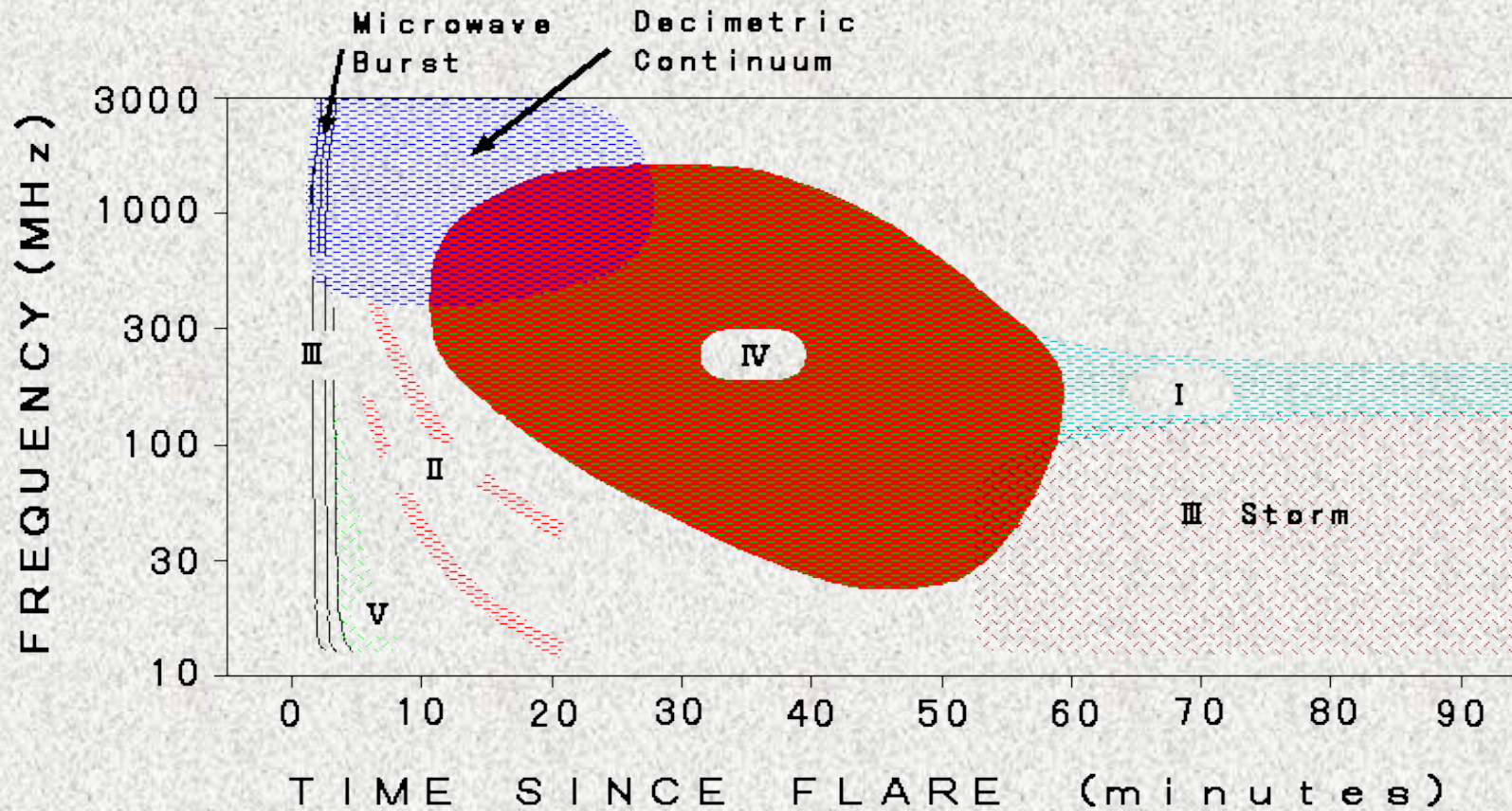
Table 1. Summary of specifications of the Log Periodic Dipole Antenna (LPDA) of Udaipur-CALLISTO.

| | |
|-----------------|---------------|
| Frequency range | 45–870 MHz |
| Gain | 8–9 dBi |
| Beam width | 90–110 degree |
| VSWR | <2 |
| Return loss | < -10 dB |

Parameters for mechanical design

| | |
|--------------------------------|-------------|
| Number of elements | 28 |
| Material for boom and elements | Aluminium |
| Length of each boom | 3.63 m |
| Cross section of each boom | 4 cm × 4 cm |
| Spacing between the booms | 1 cm |
| Total stub length | 0.937 m |

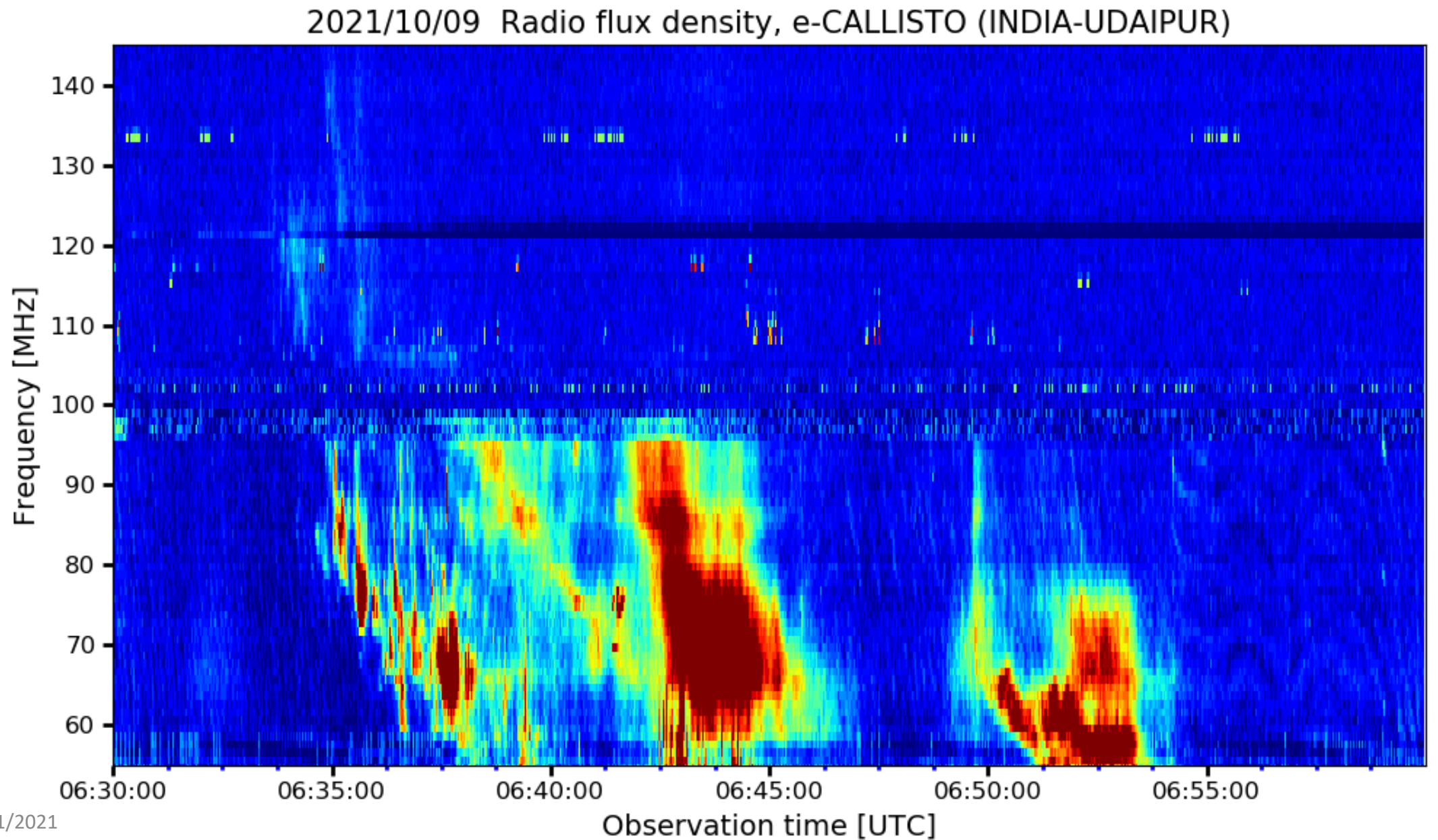
Solar radio bursts: *Flare-CME signatures in radio frequencies*



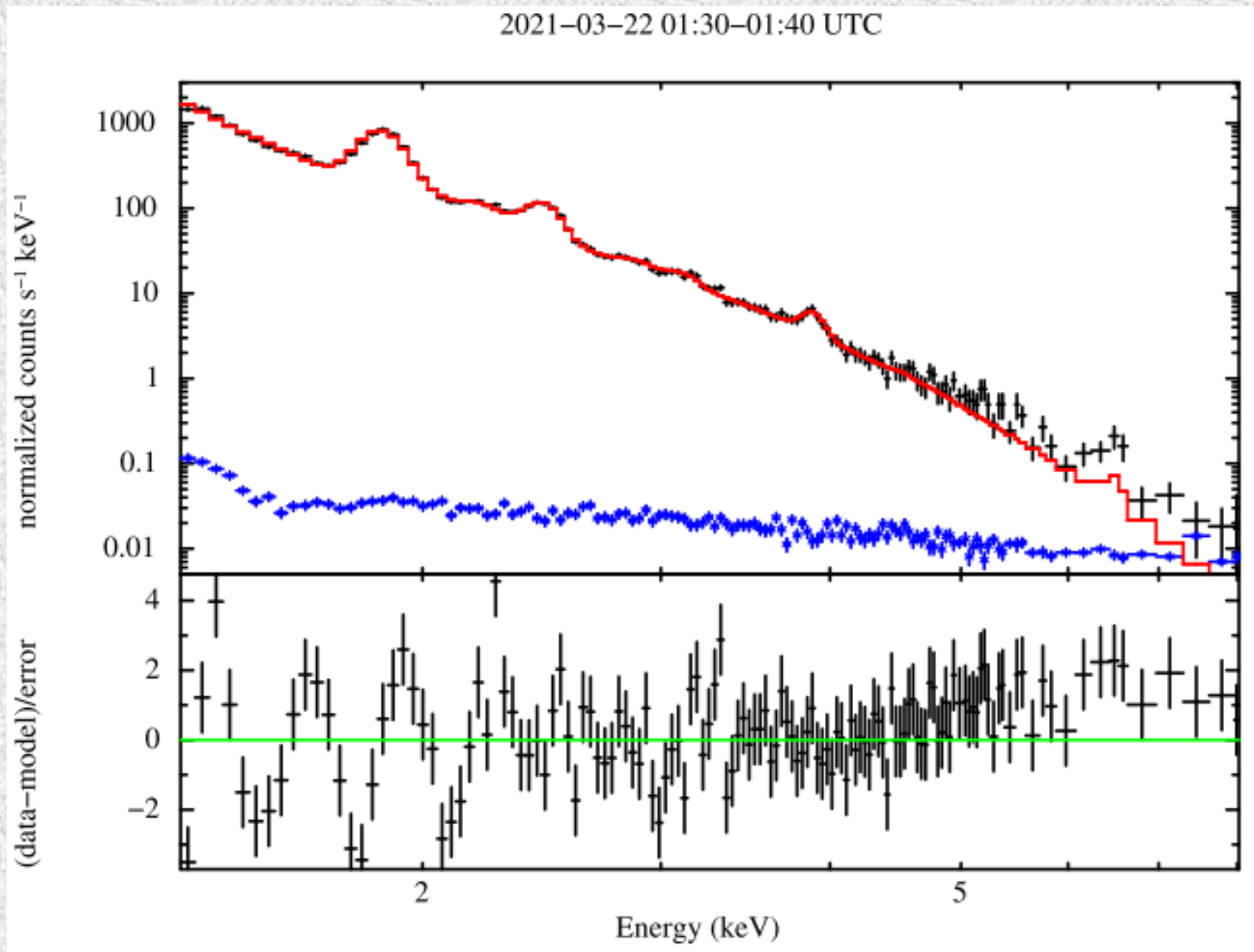
(Source: <http://sunbase.nict.go.jp/solar/denpa/index-J.html>)

- **Type I:** Due to evolution of active regions
- **Type II:** Due to shock waves
- **Type III:** Due to electron beams
- **Type IV:** Due to electrons trapped in moving or stationary magnetic structures
- **Type V:** Variant of type III

Dynamic Radio Spectrum during M-Class flare on October 9, 2021



X-ray Spectrum of a small B-class flare from XSM/Chandrayaan-2



- Mostly thermal
- Slight excess at > 5 keV
- Presence of non-thermal component ?

Concluding remarks

- ❑ Synergy between multi-wavelength observations with magnetic field measurements, extrapolations, and simulations is the key toward a better understanding of various reconnection-driven processes.
- ❑ Multi-wavelength and multi-point observations are vital to monitor the solar eruptions on real-time basis and probe the physics of flare-CME processes.